Available online at www.sciencedirect.com

SCIENCE DIRECT®

Journal of Physics and Chemistry of Solids 67 (2006) 1387–1393

JOURNAL OF
PHYSICS AND CHEMISTRY
OF SOLIDS

www.elsevier.com/locate/jpcs

Characterisation of the Ru/MgF_2 catalyst with adsorbed O_2, NO, CO probe molecules by EPR and IR spectroscopy

J. Goslar[a,*], M. Wojciechowska[b], M. Zieliński[b]

[a] Institute of Molecular Physics, Polish Academy of Sciences, Smoluchowskiego 17, 60-179 Poznań, Poland
[b] Adam Mickiewicz University, Faculty of Chemistry, Grunwaldzka 6, 60-780 Poznań, Poland

Received 15 March 2005; received in revised form 20 January 2006; accepted 25 January 2006

Abstract

Electron paramagnetic resonance (EPR) and infrared (IR) spectroscopy were used to study the formation of ruthenium and adsorbed species appearing on the catalyst during O_2, NO, and CO adsorption at room temperature on 1 wt% Ru/MgF_2 catalysts prepared from $Ru_3(CO)_{12}$. Both EPR and IR results provided clear evidence for the interaction between surface ruthenium and probe molecules. No EPR signals due to ruthenium (Ru) species were recorded at 300 and 77 K after H_2-reduction of the catalyst at 673 K. However, at 4.2 K a very weak EPR spectrum due to low-spin ($4d^5$) Ru^{3+} complexes was detected. A weak anisotropic O_2^- radicals signal with $g_{||} = 2.017$ and $g_\perp = 2.003$ superimposed on a broad ($\Delta B_{pp} = 120\,mT$), slightly asymmetric line at $g = 2.45(1)$ was identified after O_2 admission to the reduced sample. Adsorption of NO gives only a broad, Gaussian-shaped EPR line at $g = 2.43(1)$ indicating that the admission of NO, similarly to O_2 adsorption, brings about an oxidation of Ru species in the course of the NO decomposition reaction. Introduction of NO over the CO preadsorbed catalyst leads to EPR spectrum with parameters $g_\perp = 1.996$, $g_{||} = 1.895$, and $A_\perp^N = 2.9\,mT$ assigned to surface NO species associated with Ru ions. The IR spectra recorded after adsorption of NO or CO probe molecules showed the bands in the range of frequency characteristic of ruthenium nitrosyl, nitro, and nitrate/nitrite species and the bands characteristic of ruthenium mono-and multicarbonyls, respectively. Addition of CO after NO admission to the catalyst leads to appearance in the IR spectrum, beside the ones characteristic of NO adsorption, the bands which can be attributed to Ru–CO_2 and Ru–NCO species, indicating that the reaction between NO and CO occurs. These species were also detected after CO adsorption followed by NO adsorption, additionally to the band at 1850 cm^{-1} being due to *cis*–type 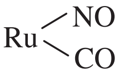 $Ru\begin{smallmatrix}\nearrow NO\\ \searrow CO\end{smallmatrix}$ species.

Keywords: A. inorganic compounds; D. surface properties

---

1. Introduction

Ruthenium-based catalysts receive continuous attention due to their role in various catalytic reactions of commercial and environmental importance [1]. Moreover, ruthenium is distinguishable among the group VIII metals being more active than platinum or rhodium [2]. In general, the cluster-derived catalysts are more active than the catalysts obtained from mononuclear complexes [3,4]. They are, for example, effective catalysts for selective production of methane from carbon dioxide and hydrogen [5], for carbon monoxide hydrogenation to alkenes [6], and for ammonia synthesis [7]. Recently, ruthenium catalysts using carbon nanotubes as support have been found to show high NH_3 conversion for the production of the CO_x–free hydrogen for proton exchange membrane fuel cells [8]. It is accepted that metal carbonyl clusters used as precursors give the well-dispersed metallic catalysts and have provided zero valent metal particles at reduction temperatures lower than conventional precursors [9]. Knowledge about the nature of surface intermediates appearing on the catalyst during probe molecules NO, CO and O_2 adsorption is of special importance for establishing the mechanism of the NO decomposition reaction, selective catalytic reduction (SCR) of NO to N_2 using hydrocarbons as reducing agents,

---

[*] Corresponding author. Tel.: +48 61 8695 219; fax: +48 61 8684 524.
E-mail address: goslarj@ifmpan.poznan.pl (J. Goslar).

0022-3697/$ - see front matter © 2006 Elsevier Ltd. All rights reserved.
doi:10.1016/j.jpcs.2006.01.106

or carbon monoxide oxidation. Highly dispersed metal species are suggested to be the active sites, however when adsorbates are added, the metal species can be coordinated to them forming surface intermediates in the reaction sequence. For example, the catalytic methanol oxidation over the catalyst has been greatly enhanced by the presence of adsorbed oxygen O^{-}_{ads} species [10]. These reaction intermediate radicals are sometimes observed directly by electron paramagnetic resonance (EPR) spectroscopy before they undergo a rapid surface reaction and become diamagnetic.

The aim of the study was to establish the surface structure of Ru/MgF_2 system. MgF_2 is a relatively new support. It is characterised by almost inert surface, good thermal stability almost up to 500 °C and high hardness. Its surface area reaches $\sim 45\,m^2/g$ and it shows a well-developed mesoporous structure (average pore diameter–$\sim$155 Å, pore volume $\sim 0.2\,cm^3/g$) [11,12]. Since magnesium fluoride does not have in its structure any oxygen atoms, differences in interaction of ruthenium with MgF_2 surface can be expected compared with interactions taking place in case of oxides such as SiO_2 or Al_2O_3. Indeed, we have found a significantly higher activity, e.g. in hydrodesulfurization (HDS) reaction of thiophene over Ru/MgF_2 catalyst containing 1.6 wt. % of ruthenium compared with Ru/SiO_2 and Ru/Al_2O_3 catalysts with the same amount of ruthenium [13].

In this paper we attempt to identify the states of the surface ruthenium sites on the MgF_2–supported $Ru_3(CO)_{12}$ catalyst and their accessibility toward various molecules. For this purpose, the adsorption of O_2, NO, and CO on the H_2–reduced Ru/MgF_2 catalyst has been studied using EPR and infrared (IR) spectroscopy to deduce the structure of the surface active sites and to establish the nature of the created species on molecular level. The application of the EPR technique is limited to the detection of the spectra due to paramagnetic species, even if they are in the minority, whereas FTIR is sensitive to all molecular species formed upon the adsorption probe molecules on the catalyst. Thus, both spectroscopes can provide a detailed description both the nature of the species and their coordination geometry because any change in the coordination sphere affects their optical or magnetic properties.

The reaction of CO and NO is one of the most important automobile exhaust control reaction. Understanding the structure and dynamical processes involved in the reactions of these two gases on the surface is one of the goals of surface science and catalysis.

2. Experimental

Ruthenium supported catalysts were prepared by impregnation of the MgF_2 with the appropriate amount of triruthenium dodecarbonyl, $Ru_3(CO)_{12}$, in ethanolic solutions, at room temperature. Following the impregnation the catalysts were dried in air at 343 K for the time of 24 h. Before any adsorption, the samples were reduced in hydrogen flow ($30\,cm^3\,min^{-1}$) for 1 h at 673 K, and then evacuated under vacuum (10^{-4} Torr) for 1 h at 523 K. Samples of Ru/MgF_2 containing 1 wt.% Ru with a dispersion of 44% and average cluster size 75 Å were used for further studies. For the purpose of EPR study adsorbate interactions the samples were exposed to O_2, CO, NO, and CO followed by NO and inversely for 0.5 h at room temperature with a gas pressure 1–5 Torr. All the gases were of ultrahigh purity.

EPR measurements were carried out on a Radiopan SE/X 2742 spectrometer (X-band) with cylindrical TM_{110} resonator and 100 kHz magnetic field modulation. EPR spectra of reduced samples before and after admission of adsorbates were recorded at room temperature and at 77 K. The g-factors describing the EPR line positions in the magnetic field were calculated as $g = 71.4484\nu/B$, where ν is the resonance frequency (in GHz) measured by HP 5340 A frequency counter, and B is the magnetic field (in mT) determined from the field markers generated by the NMR magnetometer.

The IR spectra were taken on a Bio-Rad spectrometer, model Excalibur 3000 with Fourier transform (FT-IR). The catalysts were pressed into tablets ($\sim 4\,mg/cm^2$) under a pressure of 20 MPa, and placed in a vacuum cell with windows made of KRS5. The samples were annealed at 573 K, degassed under 10^{-4} Torr for 1 h, and then cooled to RT at which the spectrum was taken. Then the gases adsorbed (NO, CO) were subsequently introduced into the cell and the spectra were taken again. The results are presented as differentiated spectra obtained after subtraction of the fundamental spectrum.

3. Results and discussion

3.1. EPR characterisation

Fig. 1 shows the EPR spectrum of the H_2- reduced 1 wt% Ru/MgF_2 catalyst recorded at 4.2 K. At room temperature and even at 77 K no resonance due to ruthenium centres could be observed. However, at 4.2 K a very weak signal was detected. This weak, highly anisotropic spectrum with three distinct g values can arise from the low-spin Ru^{3+} ($4d^5$) complexes with rhombic symmetry. EPR detection of Ru^{3+} pseudooctahedral complexes needs low temperatures because of short relaxation time T_1 at room temperature [14]. Since $\Delta B_{pp} \sim 1/T_1$, the short relaxation time causes broadening of the EPR lines giving a very broad, sometimes undetectable EPR spectrum at RT and even at 77 K, as it was in the case of our studies. The highest field line of detected EPR spectrum appears to be composed of two poorly resolved peaks with the maxima at $g_3 = 1.91$ and $g_{3'} = 1.86$, whereas two other components of the g tensor are: $g_1 = 2.50$ and $g_2 = 2.09$. Therefore, we can postulate at least two types of statistically distributed very similar nonaxial symmetry Ru^{3+} species, with g_3 sensitive to the Ru–L (L = strongly electronegative fluorine ions) bond

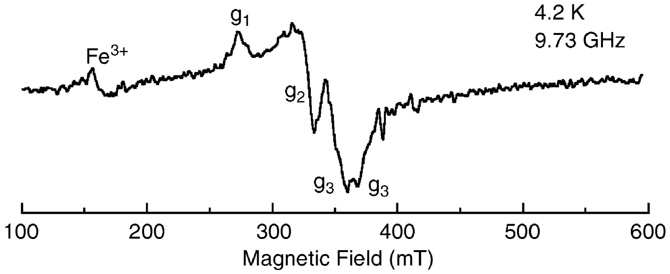

Fig. 1. EPR spectrum of 1% Ru/MgF_2 catalyst after reduction by H_2 recorded at 4.2 K, $\nu = 9.73$ GHz. A small signal at $g = 6.0\,(g_\perp^{\mathrm{eff}})$ is due to high-spin Fe^{3+} complexes of axial symmetry present in the precursors used to prepare the catalyst.

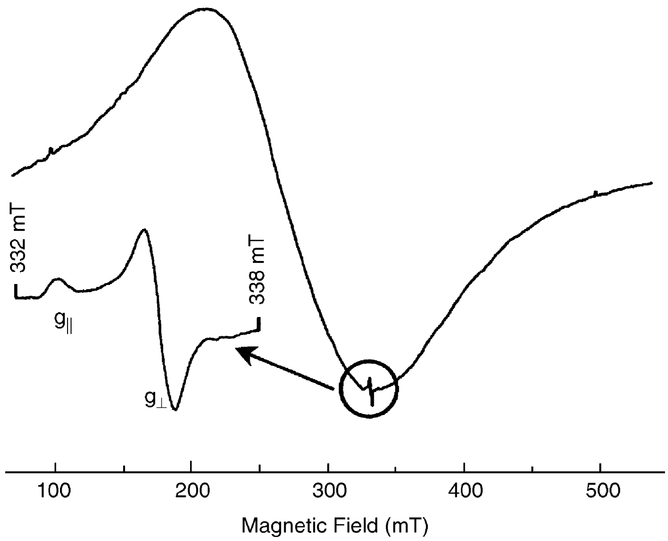

Fig. 2. EPR spectrum of Ru/MgF_2 after reaction with O_2 at room temperature, $\nu = 9.40$ GHz.

length, due to strong metal–support interactions. Large g tensor anisotropy is typical of low-spin d^5 ions in low–symmetry ligand field and, for example, rhombic symmetry complex $[Ru(NH_3)_5OH]^{2+}$ with $g_1 = 2.78$, $g_2 = 2.25$, and $g_3 = 1.62$ was observed in several types of zeolites [15–17], whereas axial spectrum with $g_x = g_y = 2.43$ and $g_z = g_{||} < 0.06$ was observed for Ru^{3+} in MgO [18] and Al_2O_3 [19]. Thus, it seems reasonable to conclude that, after the reduction treatment in a hydrogen stream, ruthenium remains on the surface mainly in metallic state (Ru^0) and as small amount of dispersed, surface Ru^{3+} species.

The EPR spectrum recorded after exposure of a reduced 1 wt% Ru/MgF_2 catalyst to O_2 at ambient temperature is shown in Fig. 2. As it is seen in the figure, this spectrum consists of a slightly asymmetric, very broad (peak-to-peak line width $\Delta B_{pp} = 120$ mT), intensive signal at $g = 2.45(1)$ and superimposed on it, a weak, anisotropic one with g tensor components $g_{zz} = g_{||} = 2.017$ and not resolved $g_{yy} = g_{xx} = g_\perp = 2.003$ (see inset of Fig. 2). These latter g tensor components are consistent with the values reported for O_2^- surface superoxides of the rhombic symmetry, detected usually in polycrystalline sample [20]. This indicates that the formation of superoxide O_2^- radical at the surface occurred by direct electron transfer from the metal cation to the adsorbed oxygen molecule and that dispersed $Ru^{x+} - (O_2^-)_{ads}$ paramagnetic species are formed with unpaired electron largely localised on the oxygen ions. The low field $g_{zz}(= g_{||})$ tensor value is the most sensitive to the nature and charge of the adsorption site [21] and is approximated to the first order by

$$g_{zz} = g_e + \frac{2\lambda}{\Delta},$$

where λ is the spin-orbit coupling constant of the oxygen ($\lambda^O = 152\,\mathrm{cm}^{-1}$) and Δ is the splitting between the two π^* orbital, one of which contains the unpaired electron, and is determined by the interaction of oxygen ion with a positive field of the adsorption cation. A well-established correlation of $g_{zz}(g_{||})$ value vs. cation charge [22] allows us to assume that O_2^- is stabilised on Ru^{4+} ions. It means that some ruthenium in interaction with O_2 could promote the formation of Ru^{4+} as well as of O_2^- superoxide, as seen by EPR.

The observed broad signal at $g = 2.45$ is presumably due to the strong dipole-dipole interaction between surface paramagnetic Ru^{x+} species produced by oxidation of the supported Ru particles, suggesting that Ru is in the form of an oxide like compound (Ru_xO_y) with Ru^{5+}/Ru^{4+} mixed valency, i.e. $S = \frac{1}{2}$ for Ru^{5+} and $S = 0$ for Ru^{4+} [23].

Only a broad, Gaussian-shaped EPR line at $g = 2.43(1)$ was detected upon contact of the Ru/MgF_2 sample with nitric oxide at room temperature indicating that the admission of NO, similarly to O_2 adsorption, brings about an oxidation of Ru species in the course of the NO decomposition reaction. This indicates that direct decomposition of NO molecules occurs on the surface reactive centres and that they are decomposed into N_2 and O_2, with the oxygen retained on the surface (on Ru sites), whereas the nitrogen is desorbed, since reaction temperature is 298 K. These reactive centres are probably the electron-rich Ru^{3+} ($4d^5$) species which can donate electrons to nitrous oxide molecules which leads to the weakening of the N–O bond, and thus to nitrous oxide decomposition. Mutual interaction between paramagnetic Ru^{x+} ions located in surface ruthenium oxide phases, as in the case of O_2, gives rise to dipolar broadening of the EPR line. From the above results, it can be concluded that ruthenium is easily oxidised by O_2 or NO forming Ru-oxide particles.

No EPR signals due to adsorbed NO molecules have been detected at room temperature and at 77 K upon contact of Ru/MgF_2 sample with nitric oxide. This fact suggests that no surface sites exist whose electric field is strong enough to remove the degeneracy of antibonding π^* orbitals of the NO molecule. Such surface sites appeared, however, after CO adsorption followed by NO adsorption on the catalyst. The EPR spectrum recorded after exposure of the reduced Ru/MgF_2 catalyst to CO and subsequent

NO adsorption at room temperature is shown in Fig. 3. After this reaction the axial symmetry signal with $g_{\perp} = 1.996$ and $g_{||} = 1.895$ and with partially resolved hyperfine structure at perpendicular peak was recorded at 77 K. Triplet of hyperfine structure with splitting $A_{\perp}^{N} = 2.9$ mT arises from interaction of the odd electron of NO with a one ^{14}N nucleus ($I = 1$). This splitting as well as g values of observed signal are very similar to those reported for nitric oxide molecules adsorbed on MgO, ZnO, and zeolites [24,25]. Thus, the detected signal is attributed to adsorption of NO on the Ru cation sites. To obtain such an EPR signal of the NO molecule, the degeneracy of the antibonding π^* orbital should be lifted by an electric field because the molecule exhibits no paramagnetism in its $^2\Pi_{1/2}$ ground state owing to the exact cancellation between the orbital magnetic moment and the spin magnetic moment of the electron. This is achieved when a molecule interacts with a strong electric field from an ion on which is adsorbed. Therefore, we may conclude that in the case of this work the NO is adsorbed on active Lewis acid site with the unpaired electron mainly localised at the NO molecule giving mixed surface ruthenium carbonyl–nitrosyl complexes, as $Ru^+(CO)_2NO$ or $Ru^+(CO)(NO)$. This agrees well with a generally accepted idea that nitric oxide is initially adsorbed on the catalyst surface and is the adsorption form of nitric oxide active in the decomposition reaction of NO in the reaction of the catalytic reduction of NO by CO [26].

Thus, under the condition of a CO and NO gas mixture, carbon monoxide interacts with the catalyst changing surface state of ruthenium and creates low co-ordinated Ru cations able to chemisorb the NO molecules, which were absent in the case of NO adsorption only.

The broad sloping baseline seen in Fig. 3 is characteristic for clustered metallic ions and is very often detected after reduction treatment leading to formation of cluster ions on the catalysts [27]. This can suggest that on Ru/MgF_2 surface Ru^0 clusters exist also during CO + NO interaction with surface of the catalyst.

3.2. IR characterisation

The adsorption of the probe molecules on H_2-reduced Ru/MgF_2 catalyst was further investigated at room temperature by FTIR spectroscopy. The infrared spectra of adsorbed species obtained upon exposure of the catalyst to NO, NO and subsequent CO, CO, and CO followed by NO are shown in Figs. 4 and 5 (spectral range 4000–500 cm^{-1}).

Upon exposure of Ru/MgF_2 catalyst to NO at room temperature, a band with a dual peak structure at 1893/1806 cm^{-1} and set of bands in the spectral range of 1700–750 cm^{-1} were recorded (Fig. 4a). Based on assignments reported previously for ruthenium nitrosyl complexes [28,29], we assigned two IR bands with maxima at around 1893 and 1806 cm^{-1} to NO molecularly adsorbed on partially oxidised Ru and metallic Ru^0 surface species, respectively (mononitrosyl ruthenium complexes $Ru^{\delta+}$–NO and Ru^0–NO). Two intense, sharp bands at 1468 and 1299 cm^{-1} accompanied by two weaker ones with maxima at 1050 and 815 cm^{-1} can be assigned to adsorbed nitrogen dioxide (–NO_2, band at 1468 cm^{-1}) and to surface ionic NO_x species such as nitrate (NO_3^-) and/or nitrite (NO_2^-) [30,31]. Although NO was adsorbed in the absence of O_2, nitrates are present on the surface, which can only be formed when gaseous NO or adsorbed NO reacts with adsorbed oxygen formed during dissociative adsorption of NO, to form NO_3^- or NO_2^- species. The charge neutrality for the formation of this species can be retained by oxidation of Ru^0 to Ru^+ and/or Ru^{3+} to Ru^{4+}. Such an oxidised process was indicated by EPR results obtained after NO adsorption as it was discussed in the previous section. The two weak adsorption peaks in the 2300–2250 cm^{-1} range are characteristic of adsorbed N_2O molecules weakly

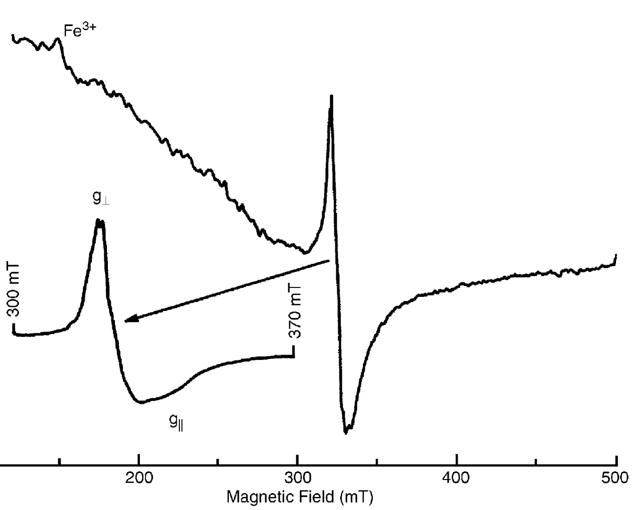

Fig. 3. EPR spectrum of NO adsorbed on Ru/MgF_2 after exposition catalyst to CO + NO recorded at 77 K, $\nu = 8.99$ GHz.

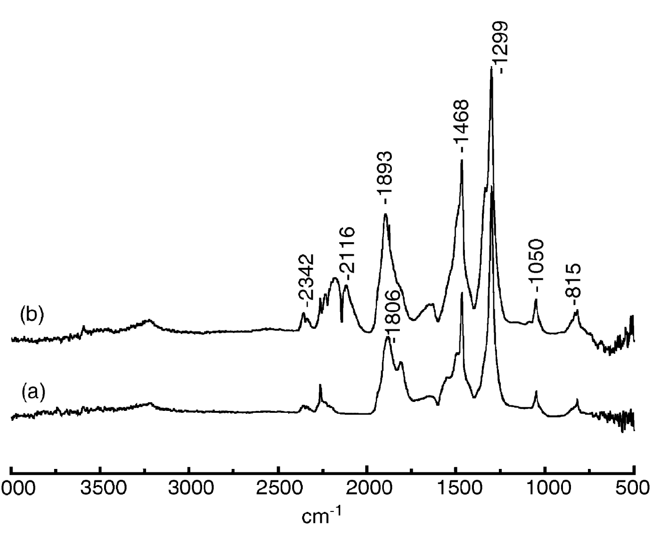

Fig. 4. Room temperature IR spectra of (a) NO adsorbed and (b) NO and CO successively adsorbed on 1 wt% Ru/MgF_2.

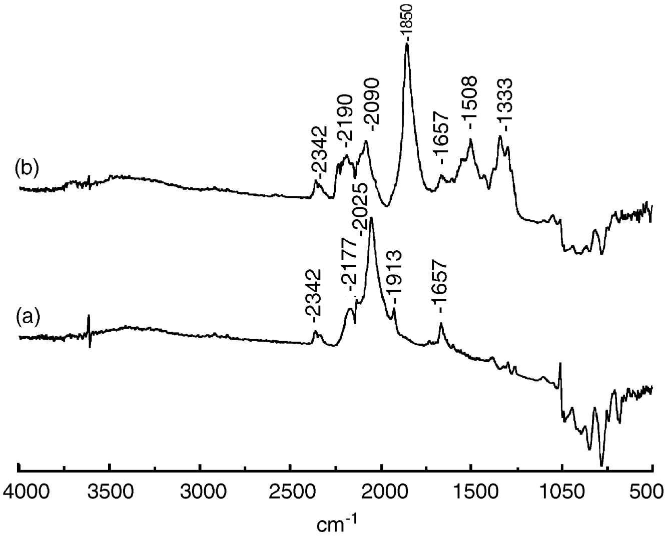

Fig. 5. Room temperature IR spectra of (a) CO adsorbed and (b) CO and NO successively adsorbed on 1 wt% Ru/MgF_2 sample.

bonded to surface and being in equilibrium with gaseous N_2O [29].

When CO was added after NO admission at 300 K, in addition to the bands that were found for separate adsorption of NO, a new IR bands in the 2400–2000 cm^{-1} range appeared as shown in Fig. 4b. Following previous literature [28,32,33] weak bands at 2342 and 2116 cm^{-1} can be related to Ru–CO_2 and Ru–isocyanate (–NCO) species, respectively. The appearance of these two surface species may indicate that the reaction NO + CO → –NCO + O occurs, and that isocyanate species react with adsorbed NO/NO_2 leading to formation N_2O and CO_2.

Room temperature CO adsorption on the reduced Ru/MgF_2 catalyst leads to the IR spectrum with absorption bands in the C–O stretch region, e.g. the intense band at 2025 cm^{-1} and three weak bands at 2342, 2177, and 1913 (Fig. 5a). According to the data reported in the literature [29,32,34], the bands at 2177 and 2025 cm^{-1} can be attributed to mononuclear $Ru^{n+}(CO)_x$ multicarbonyls ($n,x = 2$ or 3) and to CO linearly bonded to Ru^0 sites, respectively. Such bands have been observed for CO adsorption on supported ruthenium catalysts and the linear metal carbonyls are characterised by low frequency bands at 2040 ± 40, whereas the Ru^{n+}-multicarbonyls bands are expected in the high frequency region, e.g. 2180–2060 cm^{-1} [32]. The origin of $Ru^{n+}(CO)_x$ multicarbonyls after CO adsorption on reduced catalyst is not clear and has been extensively discussed in the literature. In our sample Ru^{3+} ions are present in a small amount after reduction treatment and have been detected by low temperature EPR measurements. Thus, we suggest that Ru^{3+} ions can be reduced upon contact with CO and the bis- and/or triscarbonylruthenium(II) species can be formed giving a weak band at 2177 cm^{-1} compared to a strong one at 2025 cm^{-1} due to a predominant linear adsorption of Ru^0–CO species on the surface. Kobayashi and Shirasaki proposed the formation of such species on the low coordinated Ru-atoms to explain CO adsorption on Ru/SiO_2 catalyst studied by EPR [35]. A weak band at 2342 cm^{-1} is attributed to vibration of carbon dioxide, linearly bound to the cation (Ru–C–O–O) and the appearance of this band may be taken as an indication of CO_2 formation during the adsorption of CO over catalyst. Band at 1913 cm^{-1} can be assigned to the Ru surface sites responsible for bridged adsorption of CO onto Ru^0 clusters [36,37].

Finally, we have studied the interaction of NO with CO pre-treated surface. IR spectrum showed, that the Ru–CO bands in the region of carbonyl vibrations, stable after CO contact only, are removed (CO bands at 2177 and 2025 cm^{-1} disappeared) in favour of the species stable after NO + CO contact (Fig. 5b). It can suggest that NO displaces CO as a ligand of the Ru sites forming nitrosyls. The similar nitrosyls were obtained when the catalyst was treated directly with NO. However, the peak positions and their intensity of this new spectrum (see Fig. 5b) changed and the band due to Ru–NO is now at 1850 cm^{-1} compared to 1893 cm^{-1} in the case of NO followed by CO. This shift of the NO band to a lower wave number due to surface interaction with CO can be explained as a result of the formation of *cis*-type coordinated 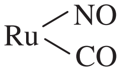 $\mathrm{Ru}\begin{smallmatrix}\nearrow \mathrm{NO}\\ \searrow \mathrm{CO}\end{smallmatrix}$ species. Similar species were found in NO reduction with CO over Ir/SiO_2 catalyst [38]. The bands assigned to NO_2, NO_3^- and NO_2^- become weaker and are shifted to a higher frequency, e.g. 1508 and 1333 cm^{-1}, respectively.

Beside this, IR spectra showed also the bands at 3250 cm^{-1} and at 1657 cm^{-1} characterising H–O–H deformations of molecularly adsorbed H_2O molecules [39].

4. Concluding remarks

Spectroscopic IR and EPR studies indicate the presence on the reduced Ru/MgF_2 catalyst both metallic Ru^0 clusters as well as incompletely reduced ruthenium particles. The reduced surface may be partially reoxidised by treatment with O_2 or NO, where N_2O and N_2 evolve in the gas phase as the products of NO decomposition:

$$NO_{gas} \rightarrow NO_{ads}$$
$$NO_{gas} \rightarrow NO_{ads} + O_{ads}$$
$$2NO_{ads} \rightarrow (N_2O)_{ads} + O_{ads}$$
$$2N_{ads} \rightarrow N_{2,gas}$$
$$2(N_2O)_{ads} \rightarrow N_{2gas} + O_{ads}$$
$$N_{ads} + NO_{ads} \rightarrow N_2O_{gas}$$

with O_{ads} retained on the surface. This oxygen and additionally formed oxygen oxidise the metal Ru^0 surface species. It is compatible with the postulated sequences of NO adsorption and desorption on ruthenium catalysts fixed on such carriers as SiO_2 [40,41], ZrO_2 [29], MgO and

Al_2O_3 [42]. It may be therefore concluded that the main role in this process is fulfilled by ruthenium, not by the carrier. Transfer of electrons from surface to adsorbed oxygen was postulated to explain O_2^- radical formation after oxygen admission. After adsorption CO followed by NO, redox type sites appeared and adducts Ru^+–NO were detected. These redox sites are the Lewis sites on which NO molecule is adsorbed to some extent affected by the crystal field existing at the adsorption site but without formal electron transfer from/or to surface. Exposure of the catalyst to CO or NO leads to the formation of ruthenium mono-and multicarbonyl complexes and to mononitrosyl $Ru^{\delta+}$–NO and Ru^0–NO complexes, respectively. The appearance in the IR spectrum of the bands assigned to nitrates, nitrites and NO_2 indicates the oxidation of NO to NO_2 and NO decomposition into O_2 and N_2. Introduction of NO over the CO preadsorbed catalyst as well as adsorption of CO on NO preadsorbed catalyst lead to IR spectra bands, which indicates that the reaction between NO and CO took place and CO_2 and isocyanate (–NCO) species were formed as follow:

$$\mathrm{NO} + \mathrm{CO} \rightarrow -\mathrm{NCO} + \mathrm{O}$$
$$-\mathrm{NCO} + \mathrm{NO} \rightarrow \mathrm{N_2} + \mathrm{CO_2}$$
$$-\mathrm{NCO} + \mathrm{NO} \rightarrow \mathrm{N_2O} + \mathrm{CO}$$
$$-\mathrm{NCO} + \mathrm{NO_2} \rightarrow \mathrm{N_2O} + \mathrm{CO_2}$$

The creation of isocyanates as transition products was also recorded for other ruthenium catalysts fixed on oxide carriers [40–42] with the exception of Ru/ZrO_2 catalyst [29]. The authors of this paper recorded carbonate species as transition products.

Thus, considering EPR and IR results, we have found that a few reactions occur on the surface of Ru/MgF_2 catalyst at room temperature depending on the adsorbed probe molecules. Moreover, the dissociative chemisorptions of NO on metallic Ru^0 occur giving rise to N_2O and CO_2 in the presence of adsorbed CO at room temperature.

Therefore,

1. On the surface of the Ru/MgF_2 catalyst ruthenium exists in a metallic and partially oxidised form.
2. The adsorption of NO leads to re-oxidation of the surface with generation of the mononitrosyl complexes. The adsorption of CO on Ru/MgF_2 gives mono-and multicarbonyl complexes.
3. The most important stage of the process NO + CO is the surface reaction between the complexes adsorbed.
4. The mechanism of NO reduction by CO occurs in the similar way as on ruthenium catalysts fixed on oxide carriers.

Acknowledgements

Michał Zieliński expressed his gratitude to the Foundation of Polish Science for fellowship.

References

[1] S. Hosokawa, H. Kanai, K. Utani, Y. Taniguchi, Y. Saito, S. Imamura, Appl. Catal. B: Environ. 45 (2003) 181 and references therein.
[2] T. Lopez, P. Bosch, M. Asomoza, R. Gomez, J. Catal. 133 (1992) 247.
[3] H.E. Ferkull, D.J. Stanton, J.D. McCowan, M.C. Baird, Can. J. Chem. 61 (1983) 1306.
[4] S. Ogura, K. Sato, Y. Inoue, Phys. Chem. Chem. Phys. 2 (2000) 2449.
[5] D.J. Darensbourg, C. Ovalles, Inorg. Chem. 25 (1986) 1603.
[6] T. Okuhara, T. Kimura, K. Kobayashi, A. Misono, Y. Yoneda, Bull. Chem. Soc. Japan 57 (1984) 938.
[7] S.E. Siporin, R.J. Davis, J. Catal. 225 (2004) 359.
[8] S.F. Yin, B.Q. Xu, W.X. Zhu, C.F. Ng, X.P. Zhou, C.T. Au, Catal. Today 93–95 (2004) 27.
[9] B.G. Johnson, M. Rameswaran, M.D. Patil, G. Muralidas, C.H. Bartholomev, Catal. Today 6 (1985) 81.
[10] T. Schedel-Niedrig, T. Neisius, I. Boettger, E. Kitzelmann, G. Weinberg, D. Demuth, R. Schloegl, Phys. Chem. Chem. Phys. 2 (2000) 2407.
[11] M. Wojciechowska, M. Zieliński, M. Pietrowski, J. Fluorine Chem. 120 (2003) 1.
[12] M. Wojciechowska, B. Czajka, M. Pietrowski, M. Zieliński, Catal. Lett. 66 (2000) 147.
[13] M. Wojciechowska, M. Pietrowski, B. Czajka, Catal. Today 65 (2001) 349.
[14] A. Abragam, B. Bleaney, Electron Paramagnetic Resonance of Transition Ions, Clarendon Press, Oxford, 1970.
[15] M. Goldwasser, J.F. Dutel, C. Naccache, Zeolites 9 (1989) 55.
[16] G.D. Lei, L. Kevan, J. Phys. Chem. 95 (1991) 4506.
[17] P.J. Carl, S.C. Larsen, J. Catal. 196 (2000) 352.
[18] A. Reizman, J.T. Suss, S. Szapiro, Solid State Commun. 9 (1971) 1799.
[19] S. Geschwind, J.P. Remeika, J. Appl. Phys. 33 (1962) 370.
[20] R.Y. Zhan, M. Narayana, L. Kevan, J. Chem. Soc. Faraday Trans. 1 81 (1985) 2083.
[21] K. Dyrek, A. Adamski, Z. Sojka, Spectrochim. Acta A 54 (1998) 2337.
[22] M. Che, A.J. Tench, Adv. Catal. 32 (1983) 1.
[23] B.L. Gustafson, M.J. Lin, J.H. Lunsford, J. Phys. Chem. 84 (1980) 3211.
[24] H. Yahiro, A. Lund, R. Aasa, N.P. Benetis, M. Shiotani, J. Phys. Chem. A 104 (2000) 7950.
[25] A. Gutsze, M. Plato, H.G. Karge, F. Witzel, J. Chem. Soc. Faraday Trans. 92 (1996) 2495.
[26] K. Dam-Johansen, P.F.B. Hansen, S. Rasmussen, Appl. Catal. B: Environ. 5 (1995) 283.
[27] Z. Chang, Z. Zhu, L. Kevan, J. Phys. Chem. B 103 (1999) 9442.
[28] G.D. Lei, L. Kevan, J. Phys. Chem. 96 (1992) 350.
[29] E. Guglielminotti, F. Boccuzzi, M. Manzoli, F. Pinna, M. Scarpa, J. Catal. 192 (2000) 149.
[30] H. Miyata, S. Konishi, T. Ohno, F. Hatayama, J. Chem. Soc. Faraday Trans. 91 (1995) 1557.
[31] E. Ito, Y.J. Mergler, B.E. Nieuwenhuys, P.M. Lugt, H. Van Bekkum, C.M. van den Bleek, in Zeolite Science 1994: Recent Progress and Discussions. Studies in Surface Science and Catalysis, Elsevier, Amsterdam, vol. 98, 1995.
[32] K. Hadjiivanov, J.-C. Lavalley, J. Lamotte, F. Maugé, J. Saint-Just, M. Che, J. Catal. 176 (1998) 415.
[33] V.A. Matyshak, O.V. Krylov, Catal. Today 25 (1995) 1.
[34] V. Mazzieri, F. Coloma-Pascual, A. Arcoya, P.C. L'Argentiére, N.S. Fígoli, Appl. Surf. Sci. 210 (2003) 222.
[35] M. Kobayashi, T. Shirasaki, J. Catal. 32 (1974) 254.
[36] K. Asakura, K.-K. Bando, Y. Iwasawa, J. Chem. Soc. Faraday Trans. 86 (1990) 2645.

[37] C. Elmasides, D.I. Kondarides, W. Grunert, X.E. Verykios, J. Phys. Chem. B 103 (1999) 5227.

[38] M. Haneda, k. Pusparatu, Y. Kintaichi, I. Nakamura, M. Sasaki, T. Fujitani, H. Hamada, J. Catal. 229 (2005) 197.

[39] J. Haber, M. Wojciechowska, J. Catal. 110 (1988) 23.

[40] A.A. Davydov, A.T. Bell, J. Catal. 49 (1977) 345.

[41] M.F. Brown, R.D. Gonzalez, J. Catal. 44 (1976) 477.

[42] A. Hornung, M. Muhler, G. Ertl, Top. Catal. 11/12 (2000) 263.